How COVID-19 related policies reshaped organic aerosol source contributions in central London

Gang I. Chen[1]*, Anja H. Tremper[1], Max Priestman[1], Anna Font[2], and David C. Green[1,3]

[1]MRC Centre for Environment and Health, Environmental Research Group, Imperial College London, 86 Wood Lane, London, W12 0BZ, UK

[2]IMT Nord Europe, Europe, Institut Mines-Télécom, Univ. Lille, Centre for Education, Research and Innovation in Energy Environment (CERI EE), 59000 Lille, France

[3]HPRU in Environmental Exposures and Health, Imperial College London, 86 Wood Lane, London, W12 0BZ, UK

*Correspondence to: Gang I. Chen (gang.chen@imperial.ac.uk)

Abstract

Particulate matter (PM) poses both health and climate risks. Understanding pollution sources is therefore crucial for effective mitigation. Positive Matrix Factorization (PMF) of Aerosol Chemical Speciation Monitor (ACSM) data is a powerful tool to quantify organic aerosol (OA) sources. A year-long study of ACSM data from London's Marylebone Road monitoring station during the COVID-19 pandemic provides insights into the impact of lockdown and the Eat Out To Help Out (EOTHO) scheme, which offered support to the hospitality industry during the pandemic, on PM composition and OA sources. Five OA sources were identified including hydrocarbon-like OA (HOA, traffic-related, 11% to OA), cooking OA (COA, 20%), biomass burning OA (BBOA, 12%), more-oxidized oxygenated OA (MO-OOA, 38%), and less-oxidized oxygenated OA (LO-OOA, 21%). Lockdown significantly reduced HOA (-52%), COA (-67%), and BBOA (-~~41~~42%) compared to their pre-COVID levels, while EOTHO ~~increased~~ doubled COA (+~~38~~100%) ~~significantly~~ compared to the post-lockdown period. However, MO-OOA and LO-OOA were less affected, as these primarily originated from long-range transport. This research has highlighted the importance of commercial cooking as a significant source of OA (20%) and PM_1 (9%) in urban areas. The co-emission of BBOA with COA observed in Central London demonstrates a similar diurnal cycle and response to the EOTHO policy, indicating that cooking activities might be currently underestimated and contribute to urban BBOA. Therefore, more effort is required to quantify this source and develop targeted abatement policies to mitigate emissions as currently limited regulation is in force.

1 Introduction

Atmospheric particulate matter (PM) are tiny particles suspended in the air, which can not only impact the climate directly and indirectly (IPCC, 2021; Seinfeld et al., 2006), but also cause adverse health effects to human (Kelly and Fussell, 2012; World Health Organization, 2021). PM consist of various constituents, including inorganic species (metals, minerals, black carbon, nitrate, sulphate, etc.) and organic species (complex mixture of thousands of compounds). European Environment Agency has reported that 99% of urban population in Europe are still exposed to polluted air with annual $PM_{2.5}$ (PM with aerodynamic diameter smaller than 2.5 μm) concentrations exceeding the WHO air quality guideline, 5 μg/m^3 (Europe's air quality status 2024, 2024; World Health Organization, 2021). As the most health-relevant air pollutant, $PM_{2.5}$ has shown strong associations with cardiovascular and respiratory related mortalities and hospital admissions (Dominici et al., 2006; Joo et al., 2024; Pye et al., 2021; Wei et al., 2022, 2024). Several studies have demonstrated that different constituents/sources contribute to health effects differently with varying toxicities (Daellenbach et al., 2020; Kelly and Fussell, 2012; Liu et al., 2023; Vasilakopoulou et al., 2023). Therefore, targeting the specific composition/sources of PM that are most health-relevant could be the most cost-effective way to mitigate its adverse health effects.

~~Source apportionment is a common but powerful approach to identifying and quantifying the emission sources and atmospheric constituents of PM based on measurements. As the sources of inorganic species (black carbon, ammonium, nitrate, chloride, sulphate, etc.) are relatively well-studied, most of the studies are focused on deconvoluting the sources of organic aerosol (OA), which contains thousands of compounds. Positive matrix factorization (PMF) is one of the receptor models that is widely utilized in the field to conduct source apportionment analysis~~Click or tap

here to enter text.~~. Typically, an Aerodyne aerosol mass spectrometer (AMS, Aerodyne Ltd., USA,) is used to measure the time series of both inorganic and organic species of non-refractory PM, in which, organic mass spectra are used for PMF analysis. However, operating an AMS is labour-intense and expensive. In contrast, the aerosol chemical speciation monitor (ACSM, Aerodyne, Ltd., has been designed for long-term monitoring purposes with less maintenance and lower capital cost, which has gained popularity across Europe and the U.S. (https://ascent.research.gatech.edu/). demonstrated a robust protocol to conduct advanced PMF analysis on long-term ACSM datasets, which delivers high-quality and consistent source apportionment results. This study follows this standardized protocol to resolve the OA sources in London by implementing advanced PMF techniques.~~

Coronavirus disease 19 (COVID-19) started to spread rapidly worldwide since the first case was identified in Wuhan, China late in 2019. Many countries implemented measures to contain COVID cases, which significantly restricted social and economic activities. In the UK, starting from the end of Mar 26th, 2020, people were ordered to stay at home and all non-essential businesses were closed, including pubs, cafes and restaurants. Non-essential shops were allowed to open on Jun 15th, and the first national lockdown came to an end Jun 23rd, 2020. However, pubs, restaurants, and cafes were only allowed to open from July 4th, 2020. Subsequently, the Eat Out to Help Out (EOTHO) Scheme was designed to help the hospitality industry; offering a 50% meal discount up to a maximum of £10 and operated Monday to Wednesday during from Aug 3rd to Aug 31st, 2020; https://www.gov.uk/guidance/get-a-discount-with-the-eat-out-to-help-out-scheme.

The UK recorded a 2.5% drop in Gross Domestic Product (GDP) in the first quarter of 2020, partly as people reduced their own activity prior to the legally enforced lockdown measures introduced on Mar 26th. This accelerated to a 19.8% fall in GDP in April to June 2020 and household spending

fell by over 20% over this period, the largest quarterly contraction on record, which was driven by falls in spending on restaurants, hotels, transport, and recreation (ONS, 2022).

Some studies have investigated the lockdown impacts on chemical composition and sources of PM, which mainly focused on cities in China (Hu et al., 2022; Tian et al., 2021; Xu et al., 2020), a kerbside site in Toronto, Canada (Jeong et al., 2022), and an urban background site in Paris, France (Petit et al., 2021). These studies all resolved primary sources including traffic related emissions, biomass burning emissions from residential heating, cooking emissions (except Paris), and secondary sources from PMF analysis on organic aerosol (OA). Traffic and cooking emissions appeared to decrease during the lockdown in all sites, while biomass burning predominately from residential heating sources in Chinese cities increased as result of remote work and rather early lockdown measures (Jan-Feb 2020) compared to France. Secondary organic aerosol (SOA) showed a more complex phenomenon given its abundance in organic components and dynamic spatiotemporal conditions. Overall, the lockdowns resulted in decreased SOA in both northwest cities in China (Tian et al., 2021; Xu et al., 2020) and Paris (Petit et al., 2021) due to lower primary emissions, and therefore fewer SOA formation products. However, Beijing experienced a large increase in SOA concentrations due to increased fossil fuel and biomass emissions, long-range transport influences as well as favourable meteorological conditions (high RH, low wind speed and low boundary layer height) for SOA formation during the lockdown period (Hu et al., 2022). Therefore, the lockdown effects on the SOA were dependent on the abundance of primary emissions, long-range transported air masses, and meteorological conditions. To date, there are few studies that investigate how COVID-related policies could have impacted PM chemical composition and sources. Petit et al. (2021) and Gamelas et al., (2023) are only two studies in Europe. The unique COVID-related policies in the UK provided a rare opportunity to investigate

the impacts these policies had on chemical composition and OA sources. To address these issues, we used highly time resolved measurements from an air quality supersite located in the Central London from 2019 to 2020, and advanced source apportionment approaches to quantify the influence of the first lockdown and EOTHO scheme on the PM composition and OA sources. This provides unique insight into PM sources and composition in a global mega city.

2 Methodology

2.1 Air quality monitoring supersite in central London

The London Marylebone Road supersite (MY, 51.52 N, -0.15 E) is a kerbside monitoring site, one meter away from a busy 6-lane road in central London. It is a well-established air quality supersite that has consistently generated high-quality air pollution data since 1997 including mass concentration of bulk PM_1, $PM_{2.5}$, and PM_{10}, as well as PM composition including black carbon, heavy metals, nitrate (NO_3), sulphate (SO_4), ammonium (NH_4), OA, Chloride (Cl), etc. More details of this site can be found at https://uk-air.defra.gov.uk/networks/site-info?site_id=MY1.

2.2 Instrumentations

Quadrupole ACSM (Q-ACSM, Aerodyne, Ltd., Ng et al. (2011)) with a standard vaporizer provides 30-min mass loadings of chemical species within non-refractory submicron aerosol (NR-PM_1), including NH_4, NO_3, SO_4, Cl, and OA. Sampled particles are focused into a narrow beam using the aerodynamic lens and impacted on a filament surface at 600 °C, where the NR-PM_1 is vaporised and ionised instantly by an electron impact source (70eV). These ions are detected by the RGA quadrupole mass spectroscopy to provide a mass spectrum of NR-PM_1 up to a mass-to-charge ratio (*m/z*) of 148 Th. The mass concentration of different chemical species are calculated

using the fragmentation table developed by Allan et al. (2004), updated for Cl following suggestions provided by Tobler et al. (2020), and a ~~(Canagaratna et al., 2007; Matthew et al., 2008)~~ composition-dependent collection efficiency (CDCE) correction suggested by Middlebrook et al. (2012) by following the ACTRIS standard operation procedure (https://www.actris-ecac.eu/pmc-non-refractory-organics-and-inorganics). With co-located black carbon (BC) measurement using a $PM_{2.5}$ cyclone with AE33 (Aerosol Magee Scientific, Ltd.) and PM_1 measurements using FIDAS (Palas, GmbH), we conducted the mass closure for fine particles measurements. The sum of NR-PM_1 and BC (in $PM_{2.5}$) reproduces PM_1 concentrations well, with a slope of 1.13 and an R^2 of 0.73 (Fig. S1).

2.3 Sampling periods and COVID-related policies

PM_1 chemical composition from Aug 1st, 2019 to Oct 22nd, 2020, was analysed as this covered the first lockdown period (Mar 26th–23 Jun 23rd, 2020) and the EOTHO Scheme (Mon-Wed during from Aug 3rd to Aug 31st, 2020, Table 1~~Table 1~~). In order to isolate the seasonal effects on the PM chemical composition and OA sources from the COVID-related policies, we further split the data based on seasons (Table 1~~Table 1~~). In addition, deweathering analysis has been conducted using "worldmet" R package (Carslaw, 2025) to remove the meteorological effects (i.e., relative humidity, wind speed, wind direction, and air temperature) on all PM/OA species as shown in the SI (Fig. S8 and Fig. S9). Meteorological effects were considerable, especially for Pre-lockdown Spring period, while it does not change the conclusion of the effects from lockdown and EOTHO policies. Therefore, the main results presented in this study are based on the original measurements.

Table 1 Dates of the COVID-related policies in London

COVID Policies		Date
Pre-Lockdown	Summer	Aug 1st–Aug 31st, 2019
	Fall	Sep 1st–Nov 30th, 2019
	Winter	Dec 1st, 2019–Feb 28th, 2019
	Spring	Mar 1st–Mar 25th, 2020
Lockdown	Spring	Mar 26th–May 31st, 2020
	Summer	Jun 1st–Jun 23rd, 2020
Post-Lockdown	Pre-EOTHO	Jun 24th–Aug 2nd, 2020
	EOTHO	Aug 3rd–Aug 31st, 2020
	Post-EOTHO	Sep 1st–Oct 22nd, 2020

2.4 Source apportionment

Source apportionment is a common but powerful approach to identifying and quantifying the emission sources and atmospheric constituents of PM based on measurements. As the sources of inorganic species (black carbon, ammonium, nitrate, chloride, sulphate, etc.) are relatively well-studied, most of the studies are focused on deconvoluting the sources of OA, which contains thousands of compounds. Positive matrix factorization (PMF) is one of the receptor models that is widely utilized in the field to conduct source apportionment analysis (Jimenez et al., 2009; Zhang et al., 2007). Typically, an Aerodyne aerosol mass spectrometer (AMS, Aerodyne Ltd., USA, Jayne et al., 2000) is used to measure the time series of both inorganic and organic species of non-refractory PM, in which, organic mass spectra are used for PMF analysis. However, operating an AMS is labour-intense and expensive. In contrast, the aerosol chemical speciation monitor (ACSM, Aerodyne, Ltd., Fröhlich et al., 2013; Ng et al., 2011) has been designed for long-term monitoring

purposes with less maintenance and lower capital cost, which has gained popularity across Europe (Chebaicheb et al., 2024; Chen et al., 2022; Laj et al., 2024) and the U.S. (https://ascent.research.gatech.edu/, Hass-Mitchell et al., 2024; Joo et al., 2024). Chen et al. (2022) demonstrated a robust protocol to conduct advanced PMF analysis on long-term ACSM datasets, which delivers high-quality and consistent source apportionment results. This study follows this standardized protocol to resolve the OA sources in London by implementing advanced PMF techniques.

Advanced source apportionment approaches have been used in this study, including rolling ~~Positive~~ positive matrix factorization (PMF), ME-2 with random *a*-value approach, bootstrap and criteria-based selections (Canonaco et al., 2021; Chen et al., 2022). ~~has been widely deployed in source apportionment of PM components including OA from ACSM/AMS datasets collected worldwide . The PMF algorithm on environmental monitoring data was initially introduced by as follows:~~

$$\cancel{x_{ij} = \sum_{k=1}^{p} g_{ik} \times f_{kj} + e_{ij}} \qquad \cancel{(1)}$$

~~where x_{ij} is the measurement matrix (here, the time series of organic mass spectra from the ACSM at i^{th} time and j^{th} m/z), g_{ik} is the mass concentration at i^{th} time in k^{th} factor, f_{kj} is the relative intensity of jth m/z for k^{th} factor, and e_{ij} stands for the residuals for j^{th} m/z at i^{th} time, p is the number of factors. The PMF model iteratively minimises the Q value using the least-squares algorithm as:~~

$$\cancel{Q = \sum_{i=1}^{n} \sum_{j=1}^{m} \left(\frac{e_{ij}}{\sigma_{ij}}\right)^2} \qquad \cancel{(2)}$$

Formatted: Font: Italic

Formatted: Justified, Space After: 10 pt

Formatted: Don't keep with next

Formatted: English (United Kingdom)

Formatted: Justified, Space After: 10 pt

Formatted: Don't keep with next

~~where n is the number of data points, m is the total number of m/z, and σ_{ij} is the measurement uncertainty estimated before the PMF analysis at i^{th} time for j^{th} m/z.~~

~~However, PMF suffers from rotational ambiguity , which provides non-unique solutions (i.e., similar Q value with different time series and factor profiles). These solutions typically will not be equally environmentally reasonable, even with similar Q values. The multilinear engine ME-2 () is a robust approach to reduce the rotational ambiguity and can direct PMF towards environmentally reasonable solutions (both factor profiles and time series).~~

~~Here, PMF was implemented using the Source Finder v9.5.1.3 (Datalystica Ltd., Switzerland, Canonaco et al. 2013) with the ME-2 solver. The latter imposes *a priori* information on the factor solutions and/or time series. The a value (ranging from 0 to 1) represents the upper limit of the relative deviation for a factor profile (f_j) or time series (g_t) from the chosen *a priori* input profile (F_j) or time series (G_t) during the iterative least-square minimization (Equation 2), as shown in Equations 3a and 3b :~~

$$\cancel{f_j = F_j \pm a \cdot F_j} \qquad \cancel{(3a)}$$

$$\cancel{g_t = G_t \pm a \cdot G_t} \qquad \cancel{(3b)}$$

~~PMF analysis is usually performed using the whole dataset, assuming that the OA source profiles are static over the entire period, which can lead to high errors when it comes to long-term datasets with non-negligible temporal variabilities of OA chemical fingerprints. showed a considerable seasonal variability of oxygenated organic aerosol (OOA) factor profiles, especially between winter and summer in a dataset in Switzerland. first introduced the concept of rolling PMF by shortening the analysis period to a smaller time window (e.g., 14 days) and then rolling over the~~

Formatted: English (United Kingdom)

Formatted: Justified, Space After: 10 pt

Formatted: Don't keep with next

Formatted: Justified, Space After: 10 pt

Formatted: Don't keep with next

~~whole dataset with a certain step (i.e., 1 day). This technique was further refined and implemented into SoFi by , which allows the PMF model to adapt the temporal variabilities of the source profiles (e.g., biogenic versus biomass burning influences on OOA factors), which usually provides well-separated OA factors.~~

~~Bootstrapping analysis will randomly select part of the PMF input matrix and duplicates itself to recreate a matrix with the same dimension as the original PMF input matrix. The statistical and rotational uncertainties of the PMF results will then be evaluated by bootstrap and the random *a*-value approach with at least 50 repeats per rolling window .~~ The standardized protocol of rolling PMF as presented in Chen et al. (2022) was used to ensure high-quality and comparable sources of OA were retrieved in London.

Specifically, PMF was first done on four different seasons as suggested in Chen et al. (2022) to determine the optimum number of factors. A total of 5 OA factors were identified: hydrocarbon-like OA (HOA), cooking-like OA (COA), biomass burning OA (BBOA), more-oxidized OOA (MO-OOA) and less-oxidized OOA (LO-OOA). Adding an additional factor resulted in split of COA factor, decreasing it to four factors caused mixing between the MO-OOA and COA factors. Therefore, 5 factor-solution was determined across the whole year. In addition, site-specific factor profiles were derived for HOA, COA, and BBOA through a seasonal bootstrap PMF analysis for winter (Dec, Jan, and Feb) and used as constraints as suggested in Chen et al. (2022) and Via et al. (2022). However, the MY site is surrounded by many restaurants with prevalent cooking emissions. Thus, the chemical fingerprint for both HOA and COA might not be fully separated. Therefore, we constrained the trend of NO_x time series, BBOA and COA profiles from a previous winter bootstrap solution collected in London North Kensington (2015-2018, Chen et al., 2022) to retrieve environmentally reasonable results with five factors in winter data, so-called base case solution.

Then, a bootstrap resampling analysis with 100 iterations and five factors was conducted by constraining the factor profiles of HOA, COA, and BBOA from the base case with random a-value from 0.1-0.5 with step of 0.1. It results in stable factor profiles of these three primary sources as shown in ~~Figure~~Fig. S2, which shows good agreements with published reference profiles (Chen et al., 2022; Crippa et al., 2013).

Rolling PMF was conducted with a time window of 14 days and a step of 1 day ~~By~~ by constraining primary factor profiles of HOA, COA, BBOA in ~~Figure~~Fig. S2 (averaged bootstrap results) and two additional unconstrained factors with bootstrap resampling and the random a-value option (0.1-0.5, step of 0.1, 50 iterations/window).~~, rolling PMF is conducted with a time window of 14 days and a step of 1 day.~~ A criteria list including selections based on both time series and factor profiles as shown in Table S1 was applied as per Chen et al. (2022). With the help of *t-test* in temporal-based criteria (1-3), we can minimize subjective judgements in determining the environmentally reasonable results. Eventually, 3,166 runs (14.1%) of the PMF runs were selected across different rolling windows across the whole year to average as the final results (utilized a-values were averaged to two decimal places) with 4.9 % unmodelled data points, which is comparable with other rolling PMF analyses (Chen et al., 2022).

Formatted: Font: Italic

3 Results and Discussions

3.1 Chemical composition of submicron PM for different periods around the COVID-19 Lockdown

The average PM_1 mass concentration at MY site was 11 μg/m^3 for the study period with 44% OA, 21% NO_3, 15% SO_4, 16% BC, 5% NH_4, and 0.6% Cl. The distribution of the chemical composition

on PM_1 varied depending on the season and variation was associated with the lockdown and EOTHO policies (Figure 1~~Figure 1~~). PM_1 increased by ~~34~~95% in lockdown spring (Mar 26th–May 31st, 2020) compared to pre-lockdown spring (Mar 1st–Mar 25th, 2020~~),~~). Specifically, Org, SO_4, ~~as well as NO_3~~ NO_3, ~~and~~ NH_4, and Cl all increased by 87%, 211%, 73%, 237%, and 132%, respectively. Except for BC, which decreased by 52%. This is due to~~the later most likely~~ ~~originated from~~the polluted airmass originating from mainland Europe and the enhanced agricultural emissions in spring from the UK and wider continental Europe (Aksoyoglu et al., 2020). It was further confirmed, through back trajectory analysis, that elevated PM_1 events (Mar 25th–Mar 28th, Apr 8th–Apr 10th, and Apr 15th–Apr 17th), where the result of airmasses passing over northern continental Europe (F~~igure~~ig. ~~S3~~S6). In addition, the Org, SO_4, NO_3, NH_4, and Cl were only increased by 21%, 107%, 50%, and 28% respectively after the deweathering analysis (Fig. S8), suggesting significant meteorological influences during this period. NO_3 concentration reduced in summer 2019 and 2020 as expected compared to spring or fall seasons due to the volatility of NH_4NO_3 and lower agricultural emissions, while SO_4 concentrations increased in summer due to enhanced photochemistry (Bressi et al., 2021; Chen et al., 2022). During the lockdown in spring SO_4 concentrations remained high, which was associated with long-range transport (Fig. S7).

Formatted: Subscript

Formatted: Subscript

Formatted: Subscript

Formatted: Subscript

Formatted: Not Superscript/ Subscript

Formatted: Not Superscript/ Subscript

Formatted: Not Superscript/ Subscript

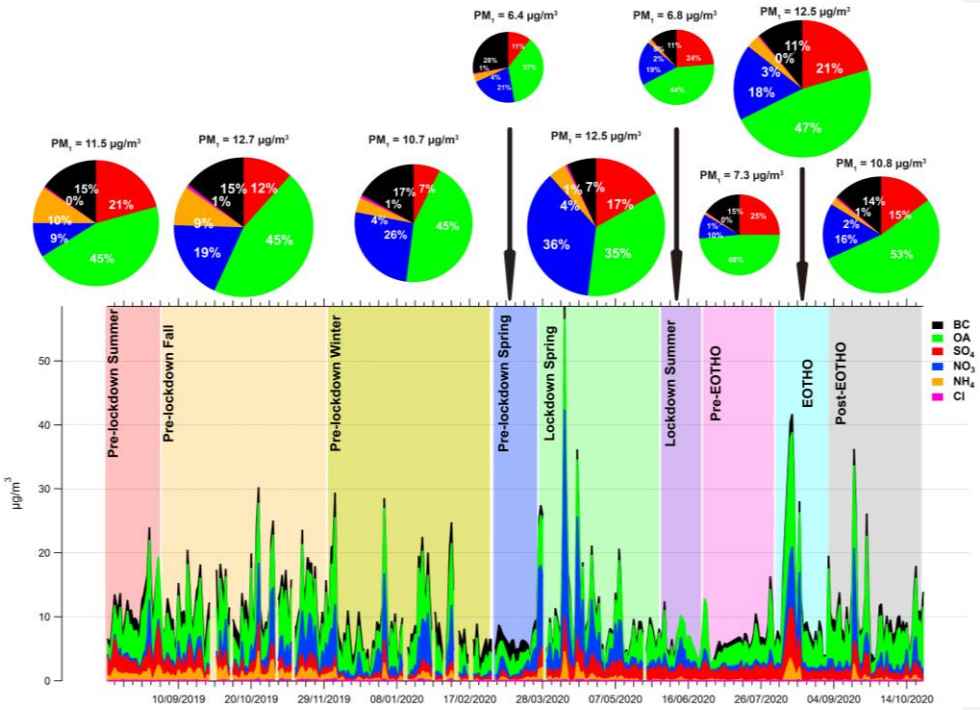

Figure 1 Chemical compositions of PM_1 at MY from Aug 2019 to Oct 2020 (daily resolution) and averaged for the different periods as shown in Table 1~~Table 1~~.

BC concentrations during the spring lockdown (Mar 26th–May 31st 2020) reduced from 1.~~59~~ 78 to 0.~~87~~ 86 µg/m^3 (-~~45~~52%) compared to the pre-lockdown level in spring (Mar 1st–Mar 25th), due to the significant reduction in traffic during the first lockdown (Transport for London, 2020). Similar decreasing of BC has been observed elsewhere during COVID lockdown as described in introduction (Gamelas et al., 2023; Jeong et al., 2022; Petit et al., 2021; Tian et al., 2021; Xu et al., 2020). ~~-~~It is worth noting that the BC concentration had already reduced by ~~13~~33% in pre-lockdown spring (Mar 1st–Mar 25th) compared to the pre-lockdown winter. This is likely due to vehicle mileage reducing as the UK government implemented travel restrictions and advised people to work from home on Mar 16th, 2020 (Transport for London, 2020). BC increased to 1.~~24~~ 13 µg/m^3

(+~~57~~44%) after the lockdown and before the EOTHO (Jun 24th–Aug 2nd,2020, pre-EOTHO in Figure 1~~Figure 1~~) as people returned to work and travel. However, BC concentrations remained ~~31~~34% lower than the pre-lockdown summer (Aug 1st–Aug 31st, 2019) concentration of 1.~~8~~ 72 μg/m^3 (Fig. S9), which suggests that the traffic emissions reduced considerably as the fewer economic activities even after the ease of the first lockdown (e.g., suggestions of hybrid working mode, restricted international travel, reduced tourism, limited access to entertainments). BC also increased to 1.~~4~~ 35 μg/m^3 (+~~10~~19%) during the EOTHO scheme (Aug 3rd–Aug 31st, 2020). This was not only because of increased traffic emission during this period, but may also result from cooking activities (e,g, barbecuing or wood-fired cooking styles) in ~~central~~ Central London (Defra, 2023). Since the EOTHO was only in place from Mon to Wed, BC concentrations (likely due to increased traffic and cooking emissions) increased on Mon-~~Tue~~ Wed compared to post-lockdown but before EOTHO (Jun 24th–Aug 2nd, 2020) (F~~igure~~ig. ~~S4~~S10).

3.2 OA sources in Central London

As mentioned above, the rolling PMF analysis resolved 5 factor solutions, including HOA, COA, BBOA, MO-OOA, and LO-OOA as shown in Figure 3~~Figure 2~~ and Figure 4~~Figure 3~~. The left panel of Figure 3~~Figure 2~~ shows the yearly averaged factor profiles of resolved PMF factors and total OOA calculated as the sum of LO-OOA and MO-OOA. All factors show good agreements with previous studies in terms of key *m/z* tracers. In addition, as shown in Figure *2*, the contribution to total OA concentrations from HOA, BBOA, and LO-OOA was consistent at different OA concentrations. However, the contribution of COA increased as total OA concentrations increased. This suggests that cooking emissions in Central London are responsible for elevated OA concentrations, which was also the case in Athens as shown in Chen et al. (2022).

Formatted: Don't keep with next

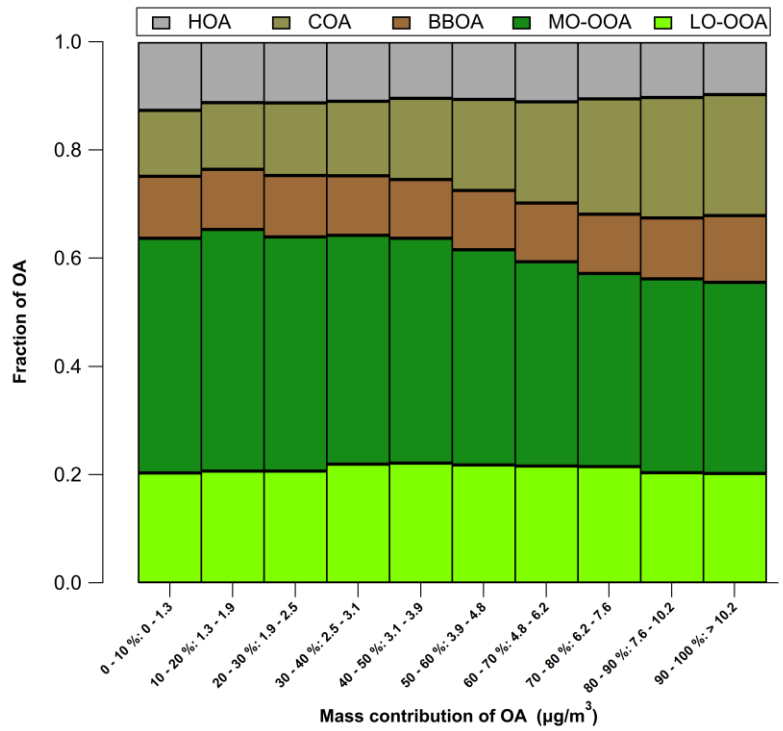

Figure 2 Contributions to total OA from the different identified OA sources at different OA concentrations. Total OA concentrations were split in 10 equally distributed bins.

~~3.2.2~~3.2.1 ~~Time series of OA factors~~General characteristics of OA factors

The right panel of Figure 3~~Figure 2~~ shows ~~both~~ time series (~~30-min time resolution~~daily averaged) and Figure 4 shows diurnal cycles for each OA factor. The mean concentrations of HOA, COA, BBOA, MO-OOA, LO-OOA, and OOA (MO-OOA+LO-OOA) were 0.50 ± 0.1 μg/m^3, 0.93 ± 0.14 μg/m^3, 0.55 ± 0.11 μg/m^3, 1.81 ± 0.41 μg/m^3, 1.00 ± 0.44 μg/m^3, and 2.80 ± 0.70 μg/m^3~~,~~ ~~respectively~~, and contributed to OA (PM_1) with the fractions of 11% (5% to PM_1), 20% (9% to PM_1), 12% (5% to PM_1), 38% (17% to PM_1), 21% (9% to PM_1), and 59% (26% to PM_1).

respectively. The concentration of all OA factors shows strong time variations over the year as shown on the ~~left panel of the~~ Figure 4~~Figure 2~~. OA factors also showed ~~strong~~ considerable seasonality besides the effects from COVID-related policies (Figure 4~~Figure 3~~ and Fig. S3). POA concentrations were generally lower in the warmer seasons than in winter as lower temperature favours particle formation via condensation and dilution and dispersion are reduced due to the lower boundary layer. It's worth mentioning that the reduced POA concentrations in warm season was not caused by reduced residential heating and energy consummation since Central London mainly uses natural gas and renewable energy instead of solid fuel combustions. The OOA factor ~~concentrations~~ concentrations remain relatively consistent across seasons, while its contributions were larger during the warmer seasons (Fig. S4). This is because ~~due to~~both ~~enhanced photochemistry~~ high temperature and strong irradiation will enhance the photochemistry and evaporation of POA sources ~~at higher temperature, stronger solar radiation~~ and the increased biogenic ~~VOC~~ volatile organic compound (VOC) emissions lead to high OOA production despite the evaporation of semi-volatile OOA (Fig. S4). The temporal variations ~~seasonality~~ observed here in central London ~~agreed~~ was consistent with the other urban sites across Europe (Chen et al., 2022). Therefore, this study focuses on the impacts of COVID-related polices on OA sources.

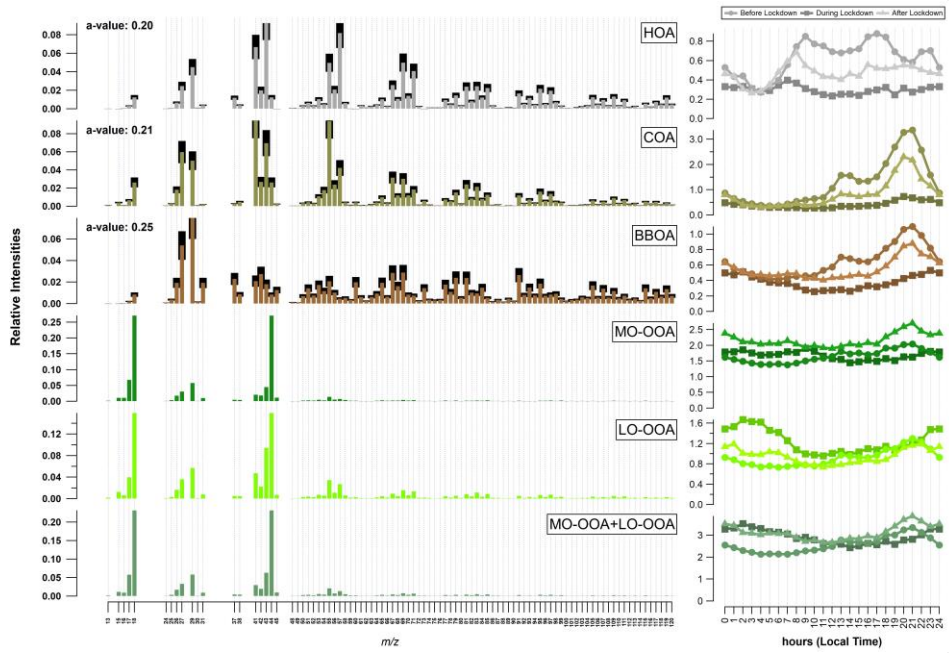

Figure 3~~2~~ Yearly averaged profiles (left) and diurnal cycles (right) of resolved factors from the rolling PMF analysis at the MY site. Time is expressed in local time.

Formatted: Centered

~~3.2.3 Diurnal Cycles for OA factors~~

The right side of Figure 3~~Figure 2~~ shows the diurnal cycles before, during, and after the lockdown. POA factors showed distinct diurnal variations, in which HOA showed morning and evening rush hour peaks, COA showed distinct lunchtime and evening peaks, and BBOA showed a similar pattern as COA before and after the lockdown. This indicates that the part of what is measured as BBOA in central London is most likely co-emitted from cooking activity, most likely from barbecuing style or wood-oven pizza restaurants in the area. A survey about use of domestic fuels in the hospitality sector was conducted by Department for Environment Food and Rural Affairs (Defra), UK suggested that restaurants use solid fuel to cook to provide unique flavours (Defra, 2023). Mohr et al. (2009) showed that meat-cooking can slightly elevate *m/z* 60, which is an

important ion in the BBOA factor profile. OOA factors showed much less diurnal variation compared to POA factors in all periods, this is in agreement with the other 22 European sites reported in Chen et al. (2022). The MO-OOA showed a smaller diurnal variation compared to LO-OOA.

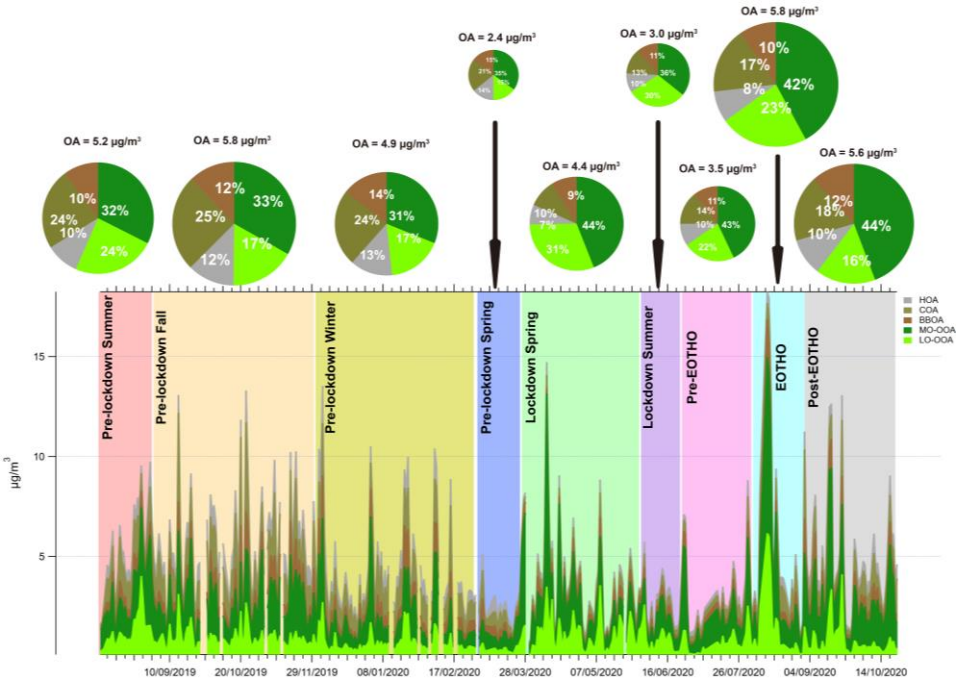

Figure ~~4~~3 Average mass concentrations for OA sources at MY during different periods from Aug 2019 to Oct 2020

Formatted: Centered

~~The diurnal variation of COA and BBOA during lockdown lost the distinctive lunch peak as shown in the pre-lockdown; and the evening peak reduced its intensity (Figure 2). HOA retained distinct morning and evening rush hour peaks but at lower mass concentrations during lockdown (Figure 2). After the first lockdown, the distinct lunch and evening peaks in diurnal patterns of COA and BBOA reappeared as the open-up of nearby restaurants. The morning and evening rush hour peaks for HOA enhanced considerably as the ease of the travel restrictions after the first lockdown.~~

~~However, POA concentrations did not reach pre-COVID levels. This is likely due to widespread hybrid working and the remaining oversea travel restrictions supressing tourism, which reduced traffic activity and restaurants visits. Conversely, OOA concentrations were slightly higher than pre-lockdown levels. These were related to long-range transport, with relatively high mass concentrations of MO-OOA and LO-OOA during the lockdown (Figure S3).~~~~As shown in Figure 4~~ ~~The contribution to total OA concentrations from HOA, BBOA, and LO-OOA was consistent at different OA concentrations. However, the contribution of COA increased as total OA~~

~~concentrations increased (Figure 4). This suggests that cooking emissions in Central London are responsible for elevated OA concentrations.~~

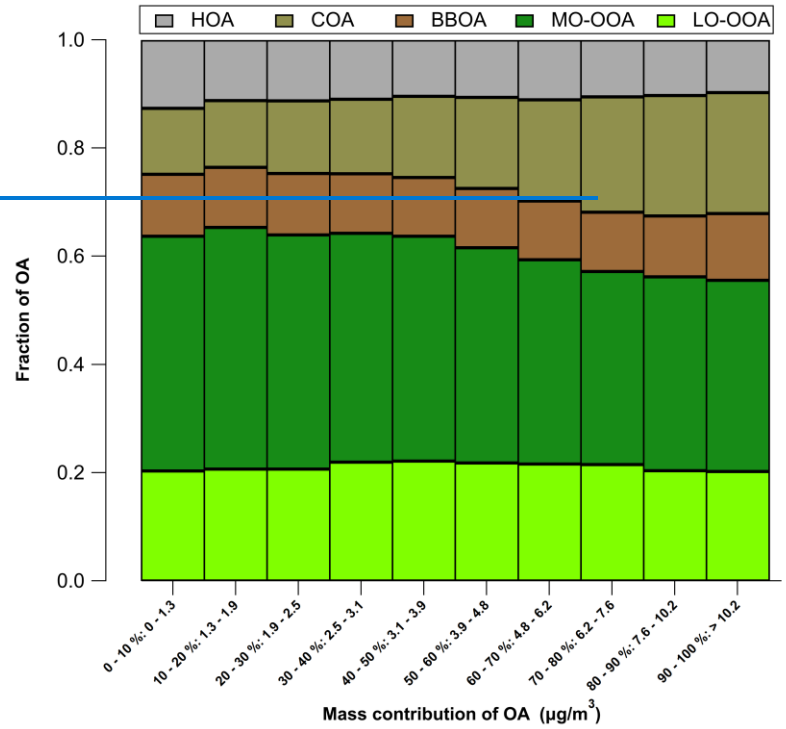

~~*Figure 4 Contributions to total OA from the different identified OA sources at different OA concentrations. Total OA concentrations were split in 10 equally distributed bins.*~~

~~As shown in Figure 4 The contribution to total OA concentrations from HOA, BBOA, and LO-OOA was consistent at different OA concentrations. However, the contribution of COA increased~~

~~as total OA concentrations increased (Figure 4), This suggests that cooking emissions in Central London are responsible for elevated OA concentrations.~~

~~Impact of lockdown on OA Concentrations~~Pre-lockdown Spring

3.2.2 Pre-lockdown Spring

~~-~~In general, OA concentration decreased by ~~34~~51%~~-~~ in pre-lockdown spring compared to pre-lockdown winter (Dec 1st, 2019–Feb 28th, 2020) due to seasonality, origins of airmass (Fig. S5), and~~-~~ ~~and~~ the impact of lockdown. OOA concentrations also decreased ~~were relatively unaffected~~ drastically ~~with some variability before, during, and after the lockdown~~by 50%.~~. due to~~ ~~long-range transportation of airmasses from the continental Europe as observed for NH_4, NO_3, and SO_4.~~ Primary emissions were significantly lower due to reduced vehicle mileage and other economic activity before the official lockdown measure came into force on March 26th 2020 (~~Figure 3 and~~ Figure 3~~Figure 2~~ (a) and Figure 4) as suggested by the 1st quarter drop in GDP (ONS, 2022). Atmospheric components related to vehicle emissions~~s~~ (HOA and BC) decreased by ~~50~~48% and ~~1~~3% respectively, in early March 2020. COA ~~and BBOA~~ decreased by ~~60~~58% ~~and 47% respectively. COA,~~ due to fewer restaurant activity, BBOA decreased by 50% was likely ~~reduced partly~~ due to the reduced commercial cooking using charcoal and wood as well as warmer weather requiring less domestic space heating.~~, and also due to reduced commercial cooking using charcoal and wood.~~

3.2.3 Lockdown

The diurnal variation of COA and BBOA during lockdown showed much less intensity overall but the distinctive lunchtime peak remained as the pre-lockdown; and the evening peak reduced its intensity (Figure 3). HOA retained distinct morning and evening rush hour peaks but at lower mass

Formatted: Superscript

Formatted: Don't keep with next

concentrations during lockdown (Figure 3). This is because the takeout activities of some restaurants were still active as well as the potential increases for residential cooking activities during lockdown. After the first lockdown, the distinct lunch and evening peaks in diurnal patterns of COA and BBOA reappeared as the open-up of nearby restaurants. The morning and evening rush hour peaks for HOA enhanced considerably as the ease of the travel restrictions after the first lockdown. However, POA concentrations did not reach pre-COVID levels (Fig. 5). This is likely due to widespread hybrid working and the remaining oversea travel restrictions supressing tourism, which reduced traffic activity and restaurants visits. Conversely, OOA concentrations during lockdown were slightly higher than pre-lockdown levels. These were related to long-range transport, with relatively high mass concentrations of MO-OOA and LO-OOA during the lockdown (Fig. S5 and Fig. S6).

Compared to the pre-lockdown spring, HOA and COA in the lockdown spring decreased by ~~8~~11% and ~~11~~15%, respectively, while BBOA increased marginally by ~~5~~13% (from 0.~~37~~35 to 0.39 μg/m^3) (Figure 5~~Figure 3~~). MO-OOA and LO-OOA increased by ~~43~~136% and ~~169~~279%, respectively due to long-range transportation of airmasses from continental Europe (Fig. S5 and Fig. S6) and increased photochemistry (enhanced temperature and ozone levels in Fig. S4) compared to the first 25 days in Mar 2020. ~~.~~This was accompanied by increased SO_4 (+~~119~~211%), NH_4 (+~~16~~132%)

and NO_3 (+~~46~~237%) as shown in Fig. S9, despite the higher temperature could favour partitioning these species into the gas phase.

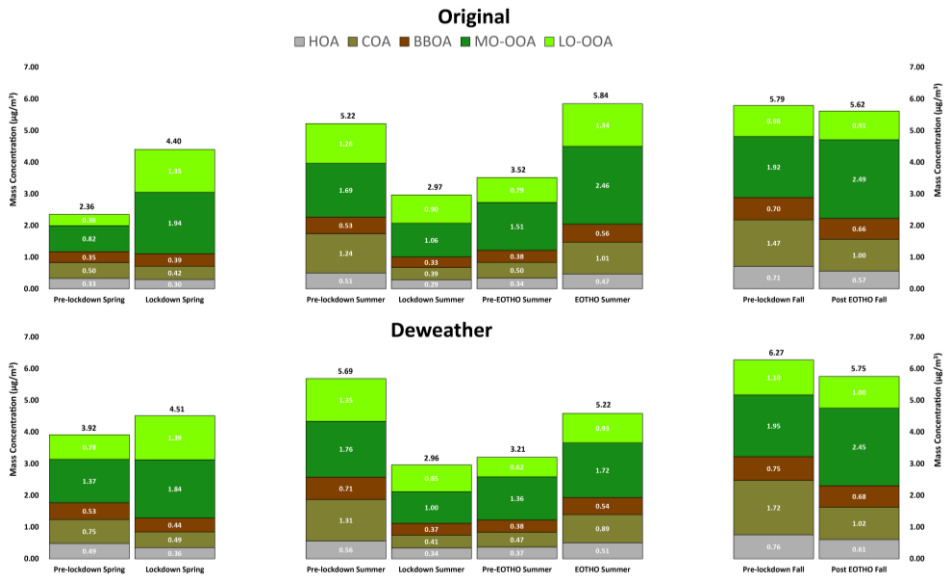

Figure 5 The impacts on OA sources during different periods compared with business-as-usual cases with and without deweathering analysis.

In June 2020, still in lockdown (Jun 1st– Jun 23rd, 2020), POA showed further but marginal decreases (-~~4~~3%, -8%, and -~~10~~15% for HOA, COA, and BBOA, respectively, Figure 4~~Figure 3~~) compared to the lockdown spring as the enhanced photochemistry leads to increased formation of OOA from the POA. However, the overall mass concentration of MO-OOA and LO-OOA decreased significantly by ~~34~~45%, and ~~37~~34%, respectively as the result of fewer long-range transported airmasses (Fig. S5).

During pre-EOTHO (Jun 24th–Aug 2nd, 2020), HOA, COA, and BBOA all showed considerably increases of ~~34~~16%, ~~69~~30%, and ~~25~~14%, respectively when compared to lockdown summer period. In which, MO-OOA ~~and LO-OOA also~~ increased by 45% and LO-OOA decreased by ~~18~~13%,

respectively as the ~~results of long-range transported airmasses from continental Europe, enhanced biogenic emissions and photochemistry~~relatively higher temperature and irradiations were favouring the vaporization of LO-OOA and production of MO-OOA from LO-OOA and POA. ~~The~~ As shown in Figure 5, the POA concentrations were much lower when compared to summer 2019 (Aug 1st–Aug 31st, 2019) as travel and economic activities did not return to pre-COVID levels (ONS, 2022; Transport for London, 2020). Specifically, reduced vehicle mileage resulted in lower HOA (-~~22~~33%), BC (-~~31~~37%), COA (-~~46~~59%) due to the reduced commercial cooking activity. As BBOA is co-emitted with COA during of cooking activities, BBOA also decreased slightly from 0.53 to 0.~~44~~ 38 μg/m^3 (-~~17~~28%, Figure 5~~Figure 3~~).

~~3.2.9~~3.2.4 Eat ~~out~~ Out ~~to~~ To ~~help~~ Help ~~out~~ Out (EOTHO)

~~During EOTHO (Aug 3rd–Aug 31st, 2020), MO-OOA and LO-OOA increased by 31% and 35% respectively compared to post-lockdown concentrations before EOTHO and correlated with increased NO_3- and SO_4- concentrations. This was due to long-ranged transported airmasses and enhanced photochemistry as well as the photooxidation of POAs.~~

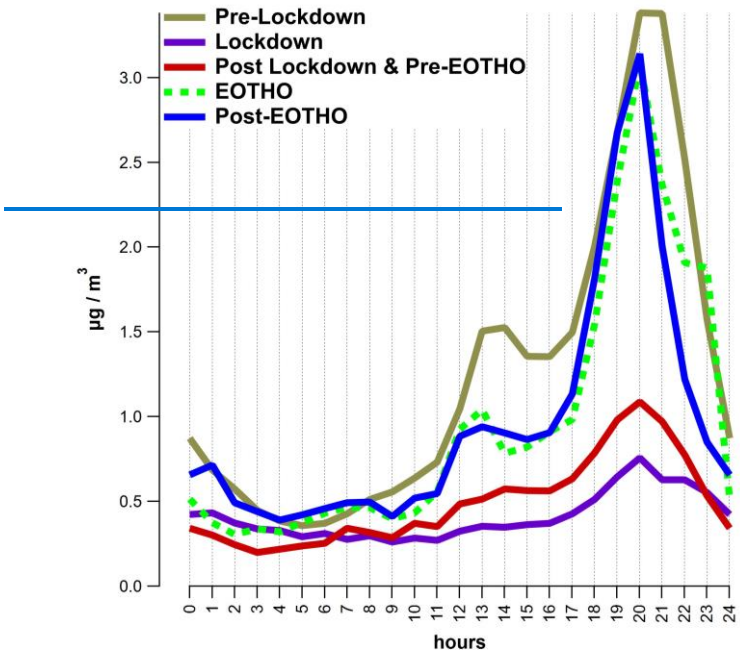

~~Figure 5 . COA diurnal plots at different periods in relation with COVID-related policies~~

~~However,~~ EOTHO policy (Aug 3rd–Aug 31st, 2020) had a significant impact on all POA factors. In particular, the COA concentration increased by ~~38~~100% compared to the post-lockdown period (Pre-EOTHO Summer) from Jun 24th to Aug 2nd, 2020 (0.5 to 1.0 µg/m^3, Figure 6~~Figure 5~~). HOA and BBOA concentrations also increased by ~~22~~40% and ~~23~~48%, respectively, which suggested the human activities resulting in these emissions recovered slowly after the lockdown (ONS, 2022; Transport for London, 2020). COA was significantly higher due to EOTHO, however, it did not reach pre-COVID concentrations (Figure 5 and Figure 6~~Figure 5~~) as its level was lower on each weekday except for Mon. ~~After the EOTHO policy (Sep 1st–Oct 22nd, 2020), COA concentrations increased by 10% (Figure 5). This may have partially been due to lower temperatures, reduced dispersion and photochemistry in Autumn.~~

Formatted: Superscript

Formatted: Not Superscript/ Subscript

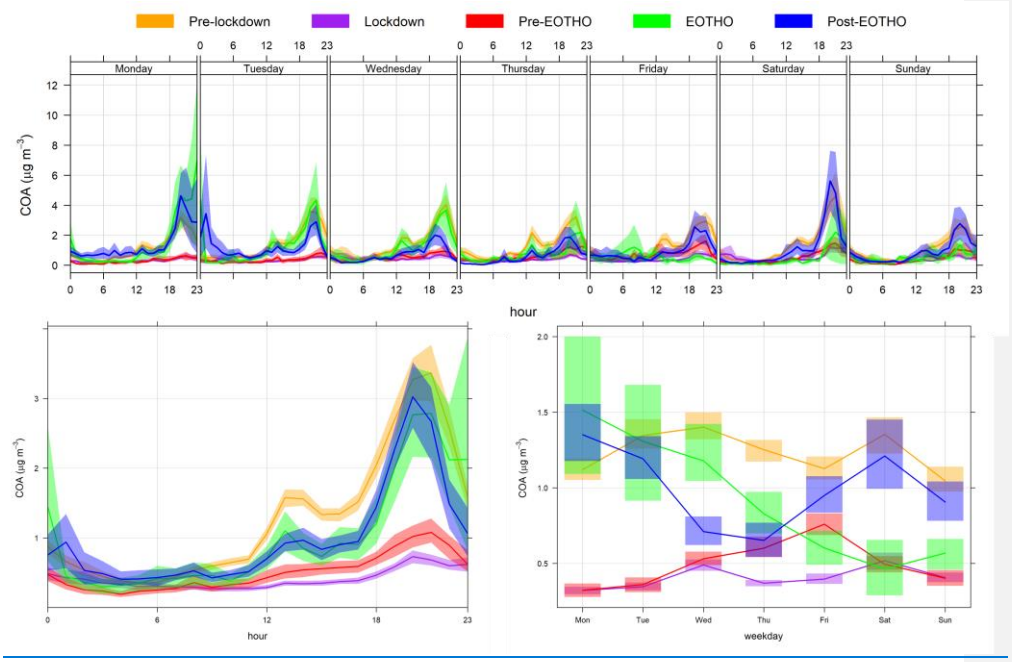

Figure 6 . COA diurnal plots for each weekday, diurnal plots, and weekly plots at different periods in relation with COVID-related policies

EOTHO only operated from Mon to Wed, and this was clear in the diurnal plots (Figure 6~~Figure 6)~~ and F~~igure~~ig. ~~S6~~ S12) with larger COA concentrations from Mon to Wed, in contrast with larger concentrations over the weekend (Fri to Sun) before EOTHO (Jun 24th–Aug 2nd, 2020). Interestingly, even after the EOTHO policy ceased (Sep 1st–Oct 22nd, 2020), COA levels remained elevated on Mon and Tue but a much higher level during the weekend was observed. This suggests that EOTHO had an influence on the consumer behaviour even after the lockdown. It is also worth noting that the high concentrations of COA and BBOA (Figure 6 and F~~igure~~ig. S~~5~~11) on Monday night were caused by the last day of EOTHO policy coinciding with a UK public holiday on Aug 31st.

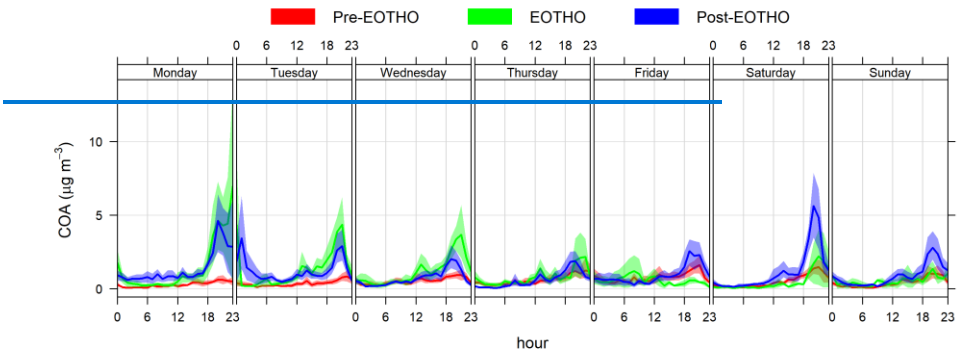

~~Figure 6 The diurnal cycles for each day of the week in COA concentrations before, during, and after the Eat Out To Help Out (EOTHO) policy in post-lockdown period (Jun 24th–Oct 22nd, 2020)~~Also, ~~D~~during EOTHO~~(Aug 3rd–Aug 31st, 2020)~~, MO-OOA and LO-OOA increased by 63% and 70% respectively compared to post-lockdown concentrations before EOTHO and correlated with increased NH_4, NO_3 and SO_4 concentrations. This was mainly due to long-ranged transported airmasses (Fig. S5) and enhanced photochemistry with increased temperature and mass concentration of POAs (Fig. S4).

~~5~~4 Conclusion

This study demonstrates the importance of source apportionment studies to better understand how national and local government policies can impact the PM mixture, and how these effects can be differentiated from the influences of meteorology and large-scale atmospheric processes. PM concentrations increased at the beginning of the lockdown (Mar–Apr 2020~~),~~) despite ~~coinciding with~~ reduced economic activities, which was caused by long-range transported airmasses instead of primary emissions~~,~~. ~~however b~~Through~~y~~ examining the source apportionment (and inorganic

Formatted: Subscript

Formatted: Normal, Left

PM composition). ~~the impact of lockdown policies on primary emissions could be quantified.~~ COVID-related policies were found to have profound but largely unintended impacts on air quality. The first lockdown significantly reduced POA sources: including HOA by 52%, COA by 67%, and BBOA by ~~41~~42%. While all these components reduced dramatically during the lockdown, they only gradually increased again and did not reach pre-COVID levels during the duration of this study (Aug 2019– Oct 2020).

Most significantly, while the Eat Out To Help Out (EOTHO) policy was effective in helping the hospitality industry to recover from economic losses during the lockdown, it had unintended impacts on air quality as cooking emissions increased. Clearly detecting this change confirms the presence of COA (20% to OA) as an important source of OA in London~~, and other cities,~~ and the importance of commercial cooking as a source. Also of note was the impact that EOTHO had on BBOA concentrations, which increased by ~~23~~48% while this policy was in place. This establishes a clear link between commercial cooking activity and BBOA measured in cities due to the use of charcoal and wood as cooking fuels (Defra, 2023), as well as potentially emissions from cooking ingredients. Cooking may therefore be underestimated as a source if COA concentrations are considered in isolation, and BBOA is only associated with other sources of solid fuel burning. This emphasises the need to develop policies and technical solutions to mitigate commercial cooking emissions in the urban environment, especially as there are limited regulations on this industry in terms of air pollution. There are filter technologies (e.g., electrostatic precipitators, UV-C lamp exhaust hood, hydrovents) available that have been implemented as law in Hong Kong to effectively control cooking emissions (Hong Kong EPD, 2024). It also demonstrated the importance in continuous monitoring with subsequent source apportionment analysis to better understand the influence of government policies to improve air quality more effectively.

489

Code/Data availability

Rolling PMF analyses is run using SoFi Pro from Datalystica (https://datalystica.com/sofi-pro/, Datalystica, 2024) under Igor Pro 9 platform from WaveMetrics® (https://www.wavemetrics.com/, WaveMetrics, 2024) and they are both available for purchase. Raw data/results from the study are available upon request to the corresponding author Gang I. Chen (gang.chen@imperial.ac.uk).

Author contribution

Gang I. Chen: Writing – review & editing, Writing – original draft, Visualization, Validation, Project administration, Methodology, Investigation, Funding acquisition, Formal analysis, Data curation, Conceptualization. **Anja H. Tremper:** Writing – review & editing, Methodology, Formal analysis, Data curation. **Max Priestman:** Methodology, Formal analysis, Data curation. **Anna Font:** Writing – review & editing, Methodology, Formal analysis, Data curation. **David C. Green:** Writing – review & editing, Supervision, Project administration, Methodology, Resources, Funding acquisition, Conceptualization.

Competing interests

The authors declare that they have no known competing financial interests or personal relationships that could have appeared to influence the work reported in this paper.

Acknowledgement

This study is part funded by the National Institute for Health Research (NIHR) Health Protection Research Unit in Environmental Exposures and Health, a partnership between UK Health Security

Agency (UKHSA) and Imperial College London. The views expressed are those of the authors and not necessarily those of the NIHR, UKHSA or the Department of Health and Social Care. This study was also supported by NERC Awards (NE/1007806/1)

References

Aksoyoglu, S., Jiang, J., Ciarelli, G., Baltensperger, U., and Prévôt, A. S. H.: Role of ammonia in European air quality with changing land and ship emissions between 1990 and 2030, Atmos Chem Phys, 20, 15665–15680, https://doi.org/10.5194/acp-20-15665-2020, 2020.

Allan, J. D., Delia, A. E., Coe, H., Bower, K. N., Alfarra, M. R., Jimenez, J. L., Middlebrook, A. M., Drewnick, F., Onasch, T. B., Canagaratna, M. R., Jayne, J. T., and Worsnop, D. R.: A generalised method for the extraction of chemically resolved mass spectra from Aerodyne aerosol mass spectrometer data, J Aerosol Sci, 35, 909–922, https://doi.org/10.1016/j.jaerosci.2004.02.007, 2004.

Bressi, M., Cavalli, F., Putaud, J. P., Fröhlich, R., Petit, J. E., Aas, W., Äijälä, M., Alastuey, A., Allan, J. D., Aurela, M., Berico, M., Bougiatioti, A., Bukowiecki, N., Canonaco, F., Crenn, V., Dusanter, S., Ehn, M., Elsasser, M., Flentje, H., Graf, P., Green, D. C., Heikkinen, L., Hermann, H., Holzinger, R., Hueglin, C., Keernik, H., Kiendler-Scharr, A., Kubelová, L., Lunder, C., Maasikmets, M., Makeš, O., Malaguti, A., Mihalopoulos, N., Nicolas, J. B., O'Dowd, C., Ovadnevaite, J., Petralia, E., Poulain, L., Priestman, M., Riffault, V., Ripoll, A., Schlag, P., Schwarz, J., Sciare, J., Slowik, J., Sosedova, Y., Stavroulas, I., Teinemaa, E., Via, M., Vodička, P., Williams, P. I., Wiedensohler, A., Young, D. E., Zhang, S., Favez, O., Minguillón, M. C., and Prevot, A. S. H.: A European aerosol phenomenology - 7: High-time resolution chemical

characteristics of submicron particulate matter across Europe, Atmos Environ X, 10, 100108, https://doi.org/10.1016/J.AEAOA.2021.100108, 2021.

Canonaco, F., Crippa, M., Slowik, J. G., Baltensperger, U., and Prévôt, A. S. H.: SoFi, an IGOR-based interface for the efficient use of the generalized multilinear engine (ME-2) for the source apportionment: ME-2 application to aerosol mass spectrometer data, Atmos Meas Tech, 6, 3649–3661, https://doi.org/10.5194/amt-6-3649-2013, 2013.

Canonaco, F., Slowik, J. G., Baltensperger, U., and Prévôt, A. S. H.: Seasonal differences in oxygenated organic aerosol composition: implications for emissions sources and factor analysis, Atmos. Chem. Phys., 15, 6993–7002, https://doi.org/10.5194/acp-15-6993-2015, 2015.

Canonaco, F., Tobler, A., Chen, G., Sosedova, Y., Slowik, J. G., Bozzetti, C., Daellenbach, K. R., El Haddad, I., Crippa, M., Huang, R.-J., Furger, M., Baltensperger, U., and Prévôt, A. S. H.: A new method for long-term source apportionment with time-dependent factor profiles and uncertainty assessment using SoFi Pro: application to 1 year of organic aerosol data, Atmos Meas Tech, 14, 923–943, https://doi.org/10.5194/amt-14-923-2021, 2021a.

Canonaco, F., Tobler, A., Chen, G., Sosedova, Y., Slowik, J. G. G., Bozzetti, C., Daellenbach, K. R., El Haddad, I., Crippa, M., Huang, R.-J., Furger, M., Baltensperger, U., Prévôt, A. S. H., Kaspar Rudolf Haddad, I. E. D., Crippa, M., Huang, R.-J., Furger, M., Baltensperger, U., Prevot, A. S. H., Daellenbach, Kaspar Rudolf Haddad, I. El, Crippa, M., Huang, R.-J., Furger, M., Baltensperger, U., and Prevot, A. S. H.: A new method for long-term source apportionment with time-dependent factor profiles and uncertainty assessment using SoFi Pro: application to 1 year of organic aerosol data, Atmos Meas Tech, 14, 923–943, https://doi.org/10.5194/amt-14-923-2021, 2021b.

deweather: Remove the influence of weather on air quality data: https://openair-project.github.io/deweather/, last access: 24 April 2025.

Chebaicheb, H., de Brito, J. F., Amodeo, T., Couvidat, F., Petit, J.-E., Tison, E., Abbou, G., Baudic, A., Chatain, M., Chazeau, B., Marchand, N., Falhun, R., Francony, F., Ratier, C., Grenier, D., Vidaud, R., Zhang, S., Gille, G., Meunier, L., Marchand, C., Riffault, V., and Favez, O.: Multiyear high-temporal-resolution measurements of submicron aerosols at 13 French urban sites: data processing and chemical composition, Earth Syst Sci Data, 16, 5089–5109, https://doi.org/10.5194/essd-16-5089-2024, 2024.

Chen, G., Sosedova, Y., Canonaco, F., Fröhlich, R., Tobler, A., Vlachou, A., Daellenbach, K. R., Bozzetti, C., Hueglin, C., Graf, P., Baltensperger, U., Slowik, J. G., El Haddad, I., and Prévôt, A. S. H.: Time-dependent source apportionment of submicron organic aerosol for a rural site in an alpine valley using a rolling positive matrix factorisation (PMF) window, Atmos Chem Phys, 21, https://doi.org/10.5194/acp-21-15081-2021, 2021.

Chen, G., Canonaco, F., Tobler, A., Aas, W., Alastuey, A., Allan, J., Atabakhsh, S., Aurela, M., Baltensperger, U., Bougiatioti, A., De Brito, J. F., Ceburnis, D., Chazeau, B., Chebaicheb, H., Daellenbach, K. R., Ehn, M., El Haddad, I., Eleftheriadis, K., Favez, O., Flentje, H., Font, A., Fossum, K., Freney, E., Gini, M., Green, D. C., Heikkinen, L., Herrmann, H., Kalogridis, A.-C., Keernik, H., Lhotka, R., Lin, C., Lunder, C., Maasikmets, M., Manousakas, M. I., Marchand, N., Marin, C., Marmureanu, L., Mihalopoulos, N., Močnik, G., Nęcki, J., O'Dowd, C., Ovadnevaite, J., Peter, T., Petit, J.-E., Pikridas, M., Matthew Platt, S., Pokorná, P., Poulain, L., Priestman, M., Riffault, V., Rinaldi, M., Różański, K., Schwarz, J., Sciare, J., Simon, L., Skiba, A., Slowik, J. G., Sosedova, Y., Stavroulas, I., Styszko, K., Teinemaa, E., Timonen, H., Tremper, A., Vasilescu, J., Via, M., Vodička, P., Wiedensohler, A., Zografou, O., Cruz Minguillón, M., and Prévôt, A. S. H.: European aerosol phenomenology − 8: Harmonised source apportionment of organic aerosol using

22 Year-long ACSM/AMS datasets, Environ Int, 166, 107325, https://doi.org/10.1016/j.envint.2022.107325, 2022.

Crippa, M., DeCarlo, P. F., Slowik, J. G., Mohr, C., Heringa, M. F., Chirico, R., Poulain, L., Freutel, F., Sciare, J., Cozic, J., Di Marco, C. F., Elsasser, M., Nicolas, J. B., Marchand, N., Abidi, E., Wiedensohler, A., Drewnick, F., Schneider, J., Borrmann, S., Nemitz, E., Zimmermann, R., Jaffrezo, J.-L., Prévôt, A. S. H., and Baltensperger, U.: Wintertime aerosol chemical composition and source apportionment of the organic fraction in the metropolitan area of Paris, Atmos Chem Phys, 13, 961–981, https://doi.org/10.5194/acp-13-961-2013, 2013.

Daellenbach, K. R., Uzu, G., Jiang, J., Cassagnes, L.-E., Leni, Z., Vlachou, A., Stefenelli, G., Canonaco, F., Weber, S., Segers, A., Kuenen, J. J. P., Schaap, M., Favez, O., Albinet, A., Aksoyoglu, S., Dommen, J., Baltensperger, U., Geiser, M., El Haddad, I., Jaffrezo, J.-L., and Prévôt, A. S. H.: Sources of particulate-matter air pollution and its oxidative potential in Europe, Nature, 587, 414–419, https://doi.org/10.1038/s41586-020-2902-8, 2020.

Defra: Use of domestic fuels in the hospitality sector – a qualitative review of hospitality businesses, 2023.

Dominici, F., Peng, R. D., Bell, M. L., Pham, L., McDermott, A., Zeger, S. L., and Samet, J. M.: Fine Particulate Air Pollution and Hospital Admission for Cardiovascular and Respiratory Diseases, JAMA, 295, 1127, https://doi.org/10.1001/jama.295.10.1127, 2006.

Efron, B.: Bootstrap Methods: Another Look at the Jackknife, The Annals of Statistics, 7, 1–26, 1979.

Europe's air quality status 2024:

Fröhlich, R., Cubison, M. J., Slowik, J. G., Bukowiecki, N., Prévôt, A. S. H., Baltensperger, U., Schneider, J., Kimmel, J. R., Gonin, M., Rohner, U., Worsnop, D. R., and Jayne, J. T.: The ToF-

ACSM: a portable aerosol chemical speciation monitor with TOFMS detection, Atmos Meas Tech, 6, 3225–3241, https://doi.org/10.5194/amt-6-3225-2013, 2013.

Gamelas, C. A., Canha, N., Vicente, A., Silva, A., Borges, S., Alves, C., Kertesz, Z., and Almeida, S. M.: Source apportionment of PM2.5 before and after COVID-19 lockdown in an urban-industrial area of the Lisbon metropolitan area, Portugal, Urban Clim, 49, 101446, https://doi.org/10.1016/j.uclim.2023.101446, 2023.

Hass-Mitchell, T., Joo, T., Rogers, M., Nault, B. A., Soong, C., Tran, M., Seo, M., Machesky, J. E., Canagaratna, M., Roscioli, J., Claflin, M. S., Lerner, B. M., Blomdahl, D. C., Misztal, P. K., Ng, N. L., Dillner, A. M., Bahreini, R., Russell, A., Krechmer, J. E., Lambe, A., and Gentner, D. R.: Increasing Contributions of Temperature-Dependent Oxygenated Organic Aerosol to Summertime Particulate Matter in New York City, ACS ES&T Air, 1, 113–128, https://doi.org/10.1021/acsestair.3c00037, 2024.

Hong Kong EPD: Control of Oily Fume and Cooking Odour from Restaurants and Food Business, 2024.

Hu, R., Wang, S., Zheng, H., Zhao, B., Liang, C., Chang, X., Jiang, Y., Yin, R., Jiang, J., and Hao, J.: Variations and Sources of Organic Aerosol in Winter Beijing under Markedly Reduced Anthropogenic Activities During COVID-2019, Environ Sci Technol, 56, 6956–6967, https://doi.org/10.1021/acs.est.1c05125, 2022.

IPCC: Climate Change 2021 – The Physical Science Basis, Cambridge University Press, https://doi.org/10.1017/9781009157896, 2021.

Jayne, J. T., Leard, D. C., Zhang, X., Davidovits, P., Smith, K. A., Kolb, C. E., and Worsnop, D. R.: Development of an Aerosol Mass Spectrometer for Size and Composition Analysis of

Submicron Particles, Aerosol Science and Technology, 33, 49–70, https://doi.org/10.1080/027868200410840, 2000.

Jeong, C.-H., Yousif, M., and Evans, G. J.: Impact of the COVID-19 lockdown on the chemical composition and sources of urban PM2.5, Environmental Pollution, 292, 118417, https://doi.org/10.1016/j.envpol.2021.118417, 2022.

Jimenez, J. L., Canagaratna, M. R., Donahue, N. M., Prevot, A. S. H. H., Zhang, Q., Kroll, J. H., DeCarlo, P. F., Allan, J. D., Coe, H., Ng, N. L., Aiken, A. C., Docherty, K. S., Ulbrich, I. M., Grieshop, A. P., Robinson, A. L., Duplissy, J., Smith, J. D., Wilson, K. R., Lanz, V. A., Hueglin, C., Sun, Y. L., Tian, J., Laaksonen, A., Raatikainen, T., Rautiainen, J., Vaattovaara, P., Ehn, M., Kulmala, M., Tomlinson, J. M., Collins, D. R., Cubison, M. J., Dunlea, J., Huffman, J. A., Onasch, T. B., Alfarra, M. R., Williams, P. I., Bower, K., Kondo, Y., Schneider, J., Drewnick, F., Borrmann, S., Weimer, S., Demerjian, K., Salcedo, D., Cottrell, L., Griffin, R., Takami, A., Miyoshi, T., Hatakeyama, S., Shimono, A., Sun, J. Y., Zhang, Y. M., Dzepina, K., Kimmel, J. R., Sueper, D., Jayne, J. T., Herndon, S. C., Trimborn, A. M., Williams, L. R., Wood, E. C., Middlebrook, A. M., Kolb, C. E., Baltensperger, U., Worsnop, D. R., Dunlea, E. J., Huffman, J. A., Onasch, T. B., Alfarra, M. R., Williams, P. I., Bower, K., Kondo, Y., Schneider, J., Drewnick, F., Borrmann, S., Weimer, S., Demerjian, K., Salcedo, D., Cottrell, L., Griffin, R., Takami, A., Miyoshi, T., Hatakeyama, S., Shimono, A., Sun, J. Y., Zhang, Y. M., Dzepina, K., Kimmel, J. R., Sueper, D., Jayne, J. T., Herndon, S. C., Trimborn, A. M., Williams, L. R., Wood, E. C., Middlebrook, A. M., Kolb, C. E., Baltensperger, U., and Worsnop, D. R.: Evolution of Organic Aerosols in the Atmosphere, Science (1979), 326, 1525–1529, https://doi.org/10.1126/science.1180353, 2009.

Joo, T., Rogers, M. J., Soong, C., Hass-Mitchell, T., Heo, S., Bell, M. L., Ng, N. L., and Gentner, D. R.: Aged and Obscured Wildfire Smoke Associated with Downwind Health Risks, Environ Sci Technol Lett, 11, 1340–1347, https://doi.org/10.1021/acs.estlett.4c00785, 2024.

Kelly, F. J. and Fussell, J. C.: Size, source and chemical composition as determinants of toxicity attributable to ambient particulate matter, Atmos Environ, 60, 504–526, https://doi.org/10.1016/j.atmosenv.2012.06.039, 2012.

Laj, P., Lund Myhre, C., Riffault, V., Amiridis, V., Fuchs, H., Eleftheriadis, K., Petäjä, T., Salameh, T., Kivekäs, N., Juurola, E., Saponaro, G., Philippin, S., Cornacchia, C., Alados Arboledas, L., Baars, H., Claude, A., De Mazière, M., Dils, B., Dufresne, M., Evangeliou, N., Favez, O., Fiebig, M., Haeffelin, M., Herrmann, H., Höhler, K., Illmann, N., Kreuter, A., Ludewig, E., Marinou, E., Möhler, O., Mona, L., Eder Murberg, L., Nicolae, D., Novelli, A., O'Connor, E., Ohneiser, K., Petracca Altieri, R. M., Picquet-Varrault, B., van Pinxteren, D., Pospichal, B., Putaud, J.-P., Reimann, S., Siomos, N., Stachlewska, I., Tillmann, R., Voudouri, K. A., Wandinger, U., Wiedensohler, A., Apituley, A., Comerón, A., Gysel-Beer, M., Mihalopoulos, N., Nikolova, N., Pietruczuk, A., Sauvage, S., Sciare, J., Skov, H., Svendby, T., Swietlicki, E., Tonev, D., Vaughan, G., Zdimal, V., Baltensperger, U., Doussin, J.-F., Kulmala, M., Pappalardo, G., Sorvari Sundet, S., and Vana, M.: Aerosol, Clouds and Trace Gases Research Infrastructure (ACTRIS): The European Research Infrastructure Supporting Atmospheric Science, Bull Am Meteorol Soc, 105, E1098–E1136, https://doi.org/10.1175/BAMS-D-23-0064.1, 2024.

Liu, F., Joo, T., Ditto, J. C., Saavedra, M. G., Takeuchi, M., Boris, A. J., Yang, Y., Weber, R. J., Dillner, A. M., Gentner, D. R., and Ng, N. L.: Oxidized and Unsaturated: Key Organic Aerosol Traits Associated with Cellular Reactive Oxygen Species Production in the Southeastern United States, Environ Sci Technol, 57, 14150–14161, https://doi.org/10.1021/acs.est.3c03641, 2023.

Middlebrook, A. M., Bahreini, R., Jimenez, J. L., and Canagaratna, M. R.: Evaluation of Composition-Dependent Collection Efficiencies for the Aerodyne Aerosol Mass Spectrometer using Field Data, Aerosol Science and Technology, 46, 258–271, https://doi.org/10.1080/02786826.2011.620041, 2012.

Mohr, C., Huffman, J. A., Cubison, M. J., Aiken, A. C., Docherty, K. S., Kimmel, J. R., Ulbrich, I. M., Hannigan, M., and Jimenez, J. L.: Characterization of primary organic aerosol emissions from meat cooking, trash burning, and motor vehicles with high-resolution aerosol mass spectrometry and comparison with ambient and chamber observations, Environ Sci Technol, 43, 2443–2449, https://doi.org/10.1021/ES8011518/SUPPL_FILE/ES8011518_SI_001.PDF, 2009.

Ng, N. L., Herndon, S. C., Trimborn, A., Canagaratna, M. R., Croteau, P. L., Onasch, T. B., Sueper, D., Worsnop, D. R., Zhang, Q., Sun, Y. L., and Jayne, J. T.: An Aerosol Chemical Speciation Monitor (ACSM) for Routine Monitoring of the Composition and Mass Concentrations of Ambient Aerosol, Aerosol Science and Technology, 45, 780–794, https://doi.org/10.1080/02786826.2011.560211, 2011a.

Ng, N. L., Canagaratna, M. R., Jimenez, J. L., Zhang, Q., Ulbrich, I. M., and Worsnop, D. R.: Real-Time Methods for Estimating Organic Component Mass Concentrations from Aerosol Mass Spectrometer Data, Environ Sci Technol, 45, 910–916, https://doi.org/10.1021/es102951k, 2011b.

ONS: GDP and events in history: how the COVID-19 pandemic shocked the UK economy, 2022.

Paatero, P.: The Multilinear Engine—A Table-Driven, Least Squares Program for Solving Multilinear Problems, Including the n -Way Parallel Factor Analysis Model, Journal of Computational and Graphical Statistics, 8, 854–888, https://doi.org/10.1080/10618600.1999.10474853, 1999.

Paatero, P. and Hopke, P. K.: Rotational tools for factor analytic models, J Chemom, 23, 91–100, https://doi.org/10.1002/cem.1197, 2009.

Paatero, P. and Tapper, U.: Positive matrix factorization: A non-negative factor model with optimal utilization of error estimates of data values, Environmetrics, 5, 111–126, https://doi.org/10.1002/env.3170050203, 1994.

Paatero, P., Hopke, P. K., Song, X.-H., and Ramadan, Z.: Understanding and controlling rotations in factor analytic models, Chemometrics and Intelligent Laboratory Systems, 60, 253–264, https://doi.org/10.1016/S0169-7439(01)00200-3, 2002.

Parworth, C., Fast, J., Mei, F., Shippert, T., Sivaraman, C., Tilp, A., Watson, T., and Zhang, Q.: Long-term measurements of submicrometer aerosol chemistry at the Southern Great Plains (SGP) using an Aerosol Chemical Speciation Monitor (ACSM), Atmos Environ, 106, 43–55, https://doi.org/10.1016/j.atmosenv.2015.01.060, 2015.

Petit, J.-E., Dupont, J.-C., Favez, O., Gros, V., Zhang, Y., Sciare, J., Simon, L., Truong, F., Bonnaire, N., Amodeo, T., Vautard, R., and Haeffelin, M.: Response of atmospheric composition to COVID-19 lockdown measures during spring in the Paris region (France), Atmos Chem Phys, 21, 17167–17183, https://doi.org/10.5194/acp-21-17167-2021, 2021.

Pye, H. O. T., Ward-Caviness, C. K., Murphy, B. N., Appel, K. W., and Seltzer, K. M.: Secondary organic aerosol association with cardiorespiratory disease mortality in the United States, Nat Commun, 12, 7215, https://doi.org/10.1038/s41467-021-27484-1, 2021.

Seinfeld, J. H., Wiley, J., and Pandis, S. N.: ATMOSPHERIC From Air Pollution to Climate Change SECOND EDITION, 628–674 pp., 2006.

Tian, J., Wang, Q., Zhang, Y., Yan, M., Liu, H., Zhang, N., Ran, W., and Cao, J.: Impacts of primary emissions and secondary aerosol formation on air pollution in an urban area of China

during the COVID-19 lockdown, Environ Int, 150, 106426, https://doi.org/10.1016/j.envint.2021.106426, 2021.

Tobler, A. K., Skiba, A., Wang, D. S., Croteau, P., Styszko, K., Nęcki, J., Baltensperger, U., Slowik, J. G., and Prévôt, A. S. H.: Improved chloride quantification in quadrupole aerosol chemical speciation monitors (Q-ACSMs), Atmos Meas Tech, 13, 5293–5301, https://doi.org/10.5194/amt-13-5293-2020, 2020.

Transport for London: Travel in London Report 13, 2020.

Vasilakopoulou, C. N., Matrali, A., Skyllakou, K., Georgopoulou, M., Aktypis, A., Florou, K., Kaltsonoudis, C., Siouti, E., Kostenidou, E., Błaziak, A., Nenes, A., Papagiannis, S., Eleftheriadis, K., Patoulias, D., Kioutsioukis, I., and Pandis, S. N.: Rapid transformation of wildfire emissions to harmful background aerosol, NPJ Clim Atmos Sci, 6, 218, https://doi.org/10.1038/s41612-023-00544-7, 2023.

Via, M., Chen, G., Canonaco, F., Daellenbach, K. R., Chazeau, B., Chebaicheb, H., Jiang, J., Keernik, H., Lin, C., Marchand, N., Marin, C., O'dowd, C., Ovadnevaite, J., Petit, J.-E., Pikridas, M., Riffault, V., Sciare, J., Slowik, J. G., Simon, L., Vasilescu, J., Zhang, Y., Favez, O., Prévôt, A. S. H., Alastuey, A., and Cruz Minguillón, M.: Rolling vs. seasonal PMF: Real-world multi-site and synthetic dataset comparison, Atmos Meas Tech, 15, https://doi.org/10.5194/amt-15-5479-2022, 2022.

Wei, Y., Qiu, X., Yazdi, M. D., Shtein, A., Shi, L., Yang, J., Peralta, A. A., Coull, B. A., and Schwartz, J. D.: The Impact of Exposure Measurement Error on the Estimated Concentration–Response Relationship between Long-Term Exposure to PM2.5 and Mortality, Environ Health Perspect, 130, https://doi.org/10.1289/EHP10389, 2022.

Wei, Y., Feng, Y., Danesh Yazdi, M., Yin, K., Castro, E., Shtein, A., Qiu, X., Peralta, A. A., Coull, B. A., Dominici, F., and Schwartz, J. D.: Exposure-response associations between chronic exposure to fine particulate matter and risks of hospital admission for major cardiovascular diseases: population based cohort study, BMJ, e076939, https://doi.org/10.1136/bmj-2023-076939, 2024.

World Health Organization: WHO global air quality guidelines. Particulate matter (PM2.5 and PM10), ozone, nitrogen dioxide, sulfur dioxide and carbon monoxide., Geneva, 2021.

Xu, J., Ge, X., Zhang, X., Zhao, W., Zhang, R., and Zhang, Y.: COVID-19 Impact on the Concentration and Composition of Submicron Particulate Matter in a Typical City of Northwest China, Geophys Res Lett, 47, https://doi.org/10.1029/2020GL089035, 2020.

Zhang, Q., Jimenez, J. L., Canagaratna, M. R., Ulbrich, I. M., Ng, N. L., Worsnop, D. R., and Sun, Y.: Understanding atmospheric organic aerosols via factor analysis of aerosol mass spectrometry: a review, Anal Bioanal Chem, 401, 3045–3067, https://doi.org/10.1007/s00216-011-5355-y, 2011.

Zhang, Qi., Jimenez, J. L., Canagaratna, M. R., Allan, J. D., Coe, H., Ulbrich, I., Alfarra, M. R., Takami, A., Middlebrook, A. M., Sun, Y. L., Dzepina, K., Dunlea, E., Docherty, K., DeCarlo, P. F., Salcedo, D., Onasch, T., Jayne, J. T., Miyoshi, T., Shimono, A., Hatakeyama, S., Takegawa, N., Kondo, Y., Schneider, J., Drewnick, F., Borrmann, S., Weimer, S., Demerjian, K., Williams, P., Bower, K., Bahreini, R., Cottrell, L., Griffin, R. J., Rautiainen, J., Sun, J. Y., Zhang, Y. M., and Worsnop, D. R.: Ubiquity and dominance of oxygenated species in organic aerosols in anthropogenically-influenced Northern Hemisphere midlatitudes, Geophys Res Lett, 34, n/a-n/a, https://doi.org/10.1029/2007GL029979, 2007.